AD_____

Award Number: W81XWH-12-1-0286

TITLE: Improving the Diagnostic Specificity of CT for Early Detection of Lung Cancer: 4D CT-Based Pulmonary Nodule Elastometry

PRINCIPAL INVESTIGATOR: Peter G. Maxim, Ph.D.

CONTRACTING ORGANIZATION: Stanford University
Stanford, CA 94305-2004

REPORT DATE: August 2013

TYPE OF REPORT: Annual

PREPARED FOR: U.S. Army Medical Research and Materiel Command
Fort Detrick, Maryland 21702-5012

REPORT DOCUMENTATION PAGE

Form Approved
OMB No. 0704-0188

1. REPORT DATE	2. REPORT TYPE	3. DATES COVERED
August 2013	Annual	15 July 2012 – 14 July 2013

4. TITLE AND SUBTITLE

Improving the Diagnostic Specificity of CT for Early Detection of Lung Cancer: 4D CT-Based Pulmonary Nodule Elastometry

5a. CONTRACT NUMBER

5b. GRANT NUMBER
W81XWH-12-1-0286

5c. PROGRAM ELEMENT NUMBER

6. AUTHOR(S)

Peter G. Maxim, Ph.D.

E-Mail: pmaxim@stanford.edu

5d. PROJECT NUMBER

5e. TASK NUMBER

5f. WORK UNIT NUMBER

7. PERFORMING ORGANIZATION NAME(S) AND ADDRESS(ES)

Stanford University
Stanford, CA 94305-2004

8. PERFORMING ORGANIZATION REPORT NUMBER

9. SPONSORING / MONITORING AGENCY NAME(S) AND ADDRESS(ES)
U.S. Army Medical Research and Materiel Command
Fort Detrick, Maryland 21702-5012

10. SPONSOR/MONITOR'S ACRONYM(S)

11. SPONSOR/MONITOR'S REPORT NUMBER(S)

12. DISTRIBUTION / AVAILABILITY STATEMENT
Approved for Public Release; Distribution Unlimited

13. SUPPLEMENTARY NOTES

14. ABSTRACT

In this study we propose to develop and validate pulmonary nodule elastometry imaging, a method complementary to CT that has the potential to increase the specificity of screening for early detection of lung cancer. We propose to address the need for greater specificity in lung cancer screening by characterizing a mechanical property of pulmonary lesions, specifically pulmonary nodule (PN) elasticity, in addition to standard anatomic features. We hypothesize that malignant and benign PN can be distinguished more specifically by different elasticities determined from 4D CT images. The specific aims of the study were the development of pulmonary nodule elastometry algorithms based on deformable image processing of 4D CT images and their validation in an animal model and in a retrospective review of over 200 4D CT scans from patients with small malignant pulmonary nodules previously treated with radiation in our department. We have successfully developed the algorithms, and in a first validation we have demonstrated proof of principles that elastometry can distinguish malignant PNs from surrounding lung tissue (a manuscript is in preparation). While this is certainly obvious, this validation has nevertheless verified the proper functioning of the algorithms. The validation in animal models and the retrospective analysis of the human data is ongoing.

15. SUBJECT TERMS
Pulmonary nodule elastometry, 4DCT, deformable image registration, Jacobian, lung cancer, lung cancer screening

16. SECURITY CLASSIFICATION OF:			17. LIMITATION OF ABSTRACT	18. NUMBER OF PAGES	19a. NAME OF RESPONSIBLE PERSON
a. REPORT	b. ABSTRACT	c. THIS PAGE			USAMRMC
U	U	U	UU	17	19b. TELEPHONE NUMBER *(include area code)*

Table of Contents

Page

Contract number: W81XWH-12-1-0286

Title: Improving the Diagnostic Specificity of CT for Early Detection of Lung Cancer: 4D CT-Based Pulmonary Nodule Elastometry

Principal Investigator: Peter G Maxim, PhD

Introduction:

In this project we are addressing a shortcoming of existing lung cancer screening methods by developing a CT based method of characterizing a mechanical property of pulmonary lesions, specifically tissue elasticity (stiffness) that should have a higher specificity than purely anatomic low-dose CT. It is the aim of the proposed study to decrease the false positive rate of CT screening by analyzing the mechanical properties of suspiciously appearing tissue during CT screening. We hypothesize that malignant pulmonary nodules are less elastic (stiffer) than benign nodules and that this difference in elasticity can be used to differentiate cancerous from benign nodules, which would help to decrease the false positive rates of CT screening. A measure of elasticity can be derived from high-resolution 4-dimensional computed tomography (4D CT) using deformable image registration algorithms. Unlike conventional 3D CT imaging that results in a static image of the scanned anatomy, 4D CT incorporates also the temporal changes of the anatomy caused by respiratory motion, yielding a CT 'movie' that allows the evaluation of tumor motion and the calculation of the elasticity.

Body:

Specific Aim 1. Development of deformable image algorithms for processing the 4D CT images to determine the elasticity of malignant and benign pulmonary nodules. *(**Dr. Maxim**, Tasks 1, months 1 – 8)*

Task 1. Development of the software for deformable image registration, analysis of the DVF and the calculation of the elasticity parameter (Matlab).

*The software will be developed using the mathematical package Matlab (The Mathworks Inc., Natick, MA). Two deformable image registration algorithms will be used (DIR^{vol} and a method based on optical flow, DIR^{OF}). The resulting displacement vector fields will be analyzed and an elasticity parameter for the pulmonary nodules will be calculated (**Dr. Maxim**, months 1 – 8).*

Status (Task 1): In addition to the two proposed deformable image registration algorithms, we also developed a third method based on a parametric nonrigid transformation model based on multi-level B-spline guided by Sum of Squared Differences (SSD) as a similarity metric. This method has proven to keep the computing time reasonably low, which is an advantage over the other methods.

$$\mathcal{T}_{\mu}(x) = x + \sum_{x_k \in \mathcal{N}_x} p_k \beta^3 \left(\frac{x - x_k}{\sigma}\right) \qquad (1)$$

with $x_k$being the control points, $\beta^3(x)$ the cubic B-spline polynomial, p_k the B-spline coefficient vectors, σ the B-spline control point spacing, and $\mathcal{N}_x$the set of all control points within the compact support of the B-spline at x. The B-spline in comparison with other spline-based transformation models, such as thin-plate spline (1-3) or elastic-body spline (4, 5), is locally controlled. One of the main motivations behind the use of B-spline transformation is the implicit regularization embedded in the B-spline basis functions, which guarantees the smoothness of transformation. The cost function, which is guided by SSD similarity metric, is minimized with respect to $\mathcal{T}$. The total cost is optimized using the gradient descent method.

The deformation gradient tensor (DGT), $\boldsymbol{F}$, maps the infinitesimal lengths between the undeformed and deformed state of a continuously deformable body:

$$\boldsymbol{F} = \begin{bmatrix} 1 + u_x & u_y & u_z \\ v_x & 1 + v_y & v_z \\ w_x & w_y & 1 + w_z \end{bmatrix} \qquad (2)$$

Various kinematic descriptors of deformation can be calculated from the DGT. Because of the need for one-to-one correspondence between material points during continuous deformation, the determinant of the DGT, normally referred to as the Jacobian, is required to be nonzero:

$$J = \det(\boldsymbol{F}) \qquad (3)$$

The degree of regional lung expansion is measured using the Jacobian of the displacement field which is directly related to specific volume change (6).

$$J = \frac{V_n + \Delta V_n}{V_n} \qquad (4)$$

where V_n is the volume of voxel element n, and ΔV_n is its change in a different respiratory cycle. A value of one implies no volumetric changes, while a Jacobian greater than one, or smaller than one implies local tissue expansion or local tissue contraction, respectively.

PN volume changes were determined by calculating the ratio of PN volume in both respiratory phases:

$$J_m = \frac{V_{inhale}^{PN}}{V_{exhale}^{PN}} \quad (4)$$

where J_m is the manually measure of volume change of PN, V_{inhale}^{PN} is the volume of the PN at deep inhale and V_{exhale}^{PN} is the volume of the PN at natural exhale.

Next, we derived an elasticity parameter defined as the ratio of the volumetric change of the PN to the volumetric change of a 1cm region of interest around the PN, **Figure 1**:

$$\zeta_{NR} = \frac{J_{GTV}}{J_{Ring}} \quad (5)$$

where J_{GTV} is the calculated volumetric change of PN and J_{Ring} is the calculated volumetric change of a 1cm region of interest around the PN. The normalization to the 1cm ROI around the PN, was introduced to remove the effect of PN location and extend of motion in the lung, as both the PN as well as the 1cm ROI will undergo the same force, irrespective to their location.

To validate the volumetric changes as determined via the Jacobian, we have manually delineated and measured the gross tumor volume (GTV) in both respiratory phases using our treatment planning software (Eclipse V11, Varian Medical Systems, Inc., Palo Alto, CA).

Specific Aim 2: Validate our method in rat models of human lung cancer and benign inflammatory lesions. *(**Dr. Maxim**, Tasks 2-4, months 3 – 24)*

Task 2. Preliminary experiments: Establish optimal protocol for the benign pulmonary model (granulomatous inflammation) and study growth kinetics.

*2a. Purchase animals: Rowett rats, A549 and SK-MES-1 cells from American Tissue Culture Collection (ATCC), carbon nanotubes (catalogue number 900–1501, lot GS1801), SES research (Houston, TX) and necessary culturing media. (**Dr. Maxim**, months 1-3)*

*2b. Inoculate 15rats (Rowett nude rats) with carbon nanotubes and follow with serial MicroCT measurements to study growth kinetics to establish the time for nodule development to reach desired size. (**Dr. Maxim**, 15 rats total, months 3 – 6)*

Task 3. Grow orthotopic model of lung cancer and benign lesions and follow with serial MicroCT imaging: preliminary experiments to establish protocol and optimize software

*3a. Inoculate 10 rats with orthotopic human lung cancer cells (A549, left lung) and carbon nanotubes (right lung) (**Dr. Maxim**, months 7-9)*

*3b. Acquire CT images at peak-inhale and peak-exhale using a small animal ventilator (**Dr. Maxim**, month 9-10)*

*3c. Analyze CT images and derive elasticity parameter and optimize software if necessary. (**Dr. Maxim**, month 10)*

Task 4. Grow orthotopic model of lung cancer and benign lesions and follow with serial MicroCT imaging, analyze data

*4a. Inoculate remaining 40 rats (A549 cells, left lung in Rowett nude rats) and follow with CT imaging at peak-inhale and peak-exhale (**Dr. Maxim**, months11-13)*

*4b. Perform simplified analysis: Delineate malignant and benign pulmonary nodules and measure volumes at peak-inhale and peak-exhale. Derive elasticity parameter based on the ratio of the volumes. (**Dr. Maxim**, months 14-15)*

*4c. Analyze acquired CT images and derive elasticity parameter by analyzing the displacement vector fields and perform statistical analysis. (**Dr. Maxim**, months 16-18)*

*4d. Repeat experiments and analysis with second cancer cell line (SK-MES-1), 50 Rowett rats, (**Dr. Maxim**, months 18-23)*

*4e. Publish animal study results (**Dr. Maxim**, month 24)*

Status (Tasks 2, 3, 4): Due to repairs and upgrades of the GE-MicroCT scanner, our proposed experiments were delayed by 4.5 months. These repairs and upgrades were unrelated to the proposed project. However, a major benefit of the upgrade was the addition of 4DCT acquisition capability, which eliminates the need of the small animal ventilator to acquire CT images at peak inhale and peak exhale. Example of acquired CT images at end inhale and exhale are shown in Figure 2.

We first aimed to establish and optimize a protocol for the pulmonary benign model**:**

Two parameters were considered in developing the protocol:

- Implanting the benign mode (carbon nanotubes) at an exact pre-determined site within the lung.
- Demonstrate that the volume of the lesion/tumor could be accurately measured at peak inhale and exhale with CT.

Six rats (6 Rowett Nude) were used in a pilot study for these parameters to develop the protocol.
Figure 3 shows the fluoroscopy images from different gantry angles showing the tip of the 1.2 cm needle near the lungs of the animals and Figure 4 shows the acquired axial CT image showing the tip of the 1.2 cm needle near the lungs.

Thus far, we were not able to to successfully generate our benign model using the carbon nantubes described in Specific Aim 2. Figure 5 shows the lungs of the animals one month after the injection of carbon nanotubes. No visible lesions were formed. One possibility is that the injection site was not within the lung parenchyma. We are modifying the injection technique to include CT confirmation of the needle tip placement prior to injection. Another possibility may be the small size of the lesions, which we intend to address by adding a gelatinous protein mixture (matrigel) to the suspension of carbon nanotubes, anticipating that the suspension will be concentrated within a specific area within the lung thereby making the lesion larger. If needed, we will utilize other agents shown to cause granulomatous inflammation. These include silica, talc, TiO_2 and other carbon nanoparticles (7, 8).
The experiments using the cancer cell lines will be initiated once we have successfully generated the benign model.

Specific Aim 3: Validate our method in a retrospective review of over 200 4D CT scans from patients previously treated in our department. *(**Dr. Loo**, Task 5 months 1 – 20)*

Task 5. Analyze approximately 200 4D CT images from previously treated patients and patients recruited within the funding period.

5a. De-archive all previously acquired thoracic 4D CT scans and identify suitable patients for the study. Our institutional data (all 4D CT scans) are currently stored on DVD's. Data will be de-archived and suitable lung cancer patients

*(patients with benign and malignant pulmonary nodules) will be identified. (**Dr. Loo**, months 1 – 3)*

5b. *Identify benign and malignant pulmonary nodules to be included in the analysis and delineate nodules at each respiratory phase. (**Dr. Loo**, month 4)*

5c. *Perform simplified analysis by calculating the ratio of the volumes with respect to peak-inhale. (**Dr. Loo**, months 5-8)*

5d. *Analyze all 4D CT images and derive elasticity parameter by analyzing the displacement vector fields and perform statistical analysis (**Dr. Loo**, months 9-15)*

5e. *Analyze data from new patients acquired during the award period (**Dr. Loo**, months 15-18).*

5f. *Publish human study results (**Dr. Loo**, months 19-20)*

Status (Task 5): Thus far, we have identified and de-archived 35 patients. Of the 35, 25 have a combination of benign and malignant nodules, 1 had multifocal malignant disease and 6 have multifocal disease and benign nodules. Adenocarcinoma represents 54.3% of the nodules, 20% squamous cell carcinoma, 20% NSCLC and 5.7% were non-diagnostic. Approximately 91.4% of the nodules were previously untreated and 8.6% are recurrent lesions. The majority of the lesions were either in the right upper lobe (28.6%), lower lobe (25.7%) or right lower lobe (20%). Dr. Loo has started with the delineation of the benign and malignant nodules. Data will be processed and analyzed shortly.

Key Research Accomplishments:

Our first aim was to develop and validate an automated software package for determining PN elasticity against a manual contouring method, and preliminarily assess its ability to distinguish malignant tissue by comparing the elasticities of malignant PN with those of the lung. Here, we have chosen an obvious case, since the elasticity of a tumor is expected to be less than that of the surrounding lung.

Figure 6 shows linear regression analysis of the manual contouring method versus the calculated Jacobian of the deformation map of the CT images derived from inhale to exhale, demonstrating that our method would match the results of a human observer. Figure 7 shows the box plot of the calculated Jacobian of a 1 cm region of interest around the tumor (ring) for 30 patients. For each box, the central mark is the median of all computed values, the edges of the box are the 25^{th} and 75^{th} percentiles, the whiskers

extend to the most extreme data points not considered outliers. These results demonstrate that our method is able to distinguish the volumetric changes of a solid tumor and its surrounding lung tissue between inhale and exhale.

In summary:

- We have developed a software package to determine the elasticity of tissue
- We have validated our software against a manual contouring method
- We have demonstrated proof of principle that our method is functioning properly, by preliminarily assessing its ability to distinguish malignant tissue from lung tissue

Reportable Outcomes:

The following abstracts have been selected for oral presentation:

1. Mohammadreza Negahdar, Billy W Loo, Maximilian Diehn, Lu Tian, Dominik Fleischmann, and Peter G Maxim, *"Automated Tool for Determining Pulmonary Nodule Elasticity to Distinguish Malignant Nodules,"* Journal of Medical Physics, 40(6), supplement for the 55th Annual Meeting of the American Association of Physicists in Medicine (AAPM), Indianapolis, IN, August 2013.

2. Mohammadreza Negahdar, Billy W Loo, Maximilian Diehn, Dominik Fleischmann, Lu Tian, and Peter G Maxim, *"Automated Pulmonary Nodule Elastometry as a Potential Diagnostic Tool,"* 99th Annual Meeting of the Radiation Society of North America (RSNA), Chicago, IL, December 2013.

A manuscript summarizing our initial validation will be submitted shortly to Int J Radiat Oncol Biol Phys.

The abstracts have been included in the 'Supporting Documentation' section.

Conclusion:

We have successfully accomplished specific aim 1 of the proposed study. We now have a functional software to process and analyze 4DCT images to distinguish malignant and benign PN. Despite setbacks in time because of upgrades of the small animal equipment and issues with the generation of a benign model in the animals, we have alternatives to our initial plan described above, thus we believe we are on track to carry out the proposed research project.

References:

1. Bookstein FL. Principal warps: thin-plate splines and the decomposition of deformations. IEEE Transactions on Pattern Analysis and Machine Intelligence. 1989;11(6):567-85.
2. Hilsmann A, Vik T, Kaus M, Franks K, Bissonette J-P, Purdie T, et al. Deformable 4DCT lung registration with vessel bifurcations. International Conference of Computer Assisted Radiology and Surgery (CARS); June. Berlin, Germany2007.
3. Rohr K, Stiehl HS, Sprengel R, Buzug TM, Weese J, Kuhn MH. Landmark-based elastic registration using approximating thin-plate splines. IEEE Transactions on Medical Imaging. 2001;20(6):526-34.
4. Davis MH, Khotanzad A, Flamig DP, Harms SE. A physics-based coordinate transformation for 3-D image matching. IEEE Transactions on Medical Imaging. 1997;16(3):317-28.
5. Wörz S, Rohr K. Physics-based elastic registration using non-radial basis functions and including landmark localization uncertainties. Computer Vision and Image Understanding. 2008;111(3):263-74.
6. Reinhardt JM, Ding K, Cao K, Christensen GE, Hoffman EA, Bodas SV. Registration-based estimates of local lung tissue expansion compared to xenon-CT measures of specific ventilation. Medical Image Analysis. 2008;12(6):752-63.
7. Castranova V, Porter D, Millecchia L, Ma JY, Hubbs AF, Teass A. Effect of inhaled crystalline silica in a rat model: time course of pulmonary reactions. Molecular and cellular biochemistry. 2002;234-235(1-2):177-84. PubMed PMID: 12162431.
8. Montes JF, Ferrer J, Villarino MA, Baeza B, Crespo M, Garcia-Valero J. Influence of talc dose on extrapleural talc dissemination after talc pleurodesis. American journal of respiratory and critical care medicine. 2003;168(3):348-55. doi: 10.1164/rccm.200207-767OC. PubMed PMID: 12773332.

Appendices:

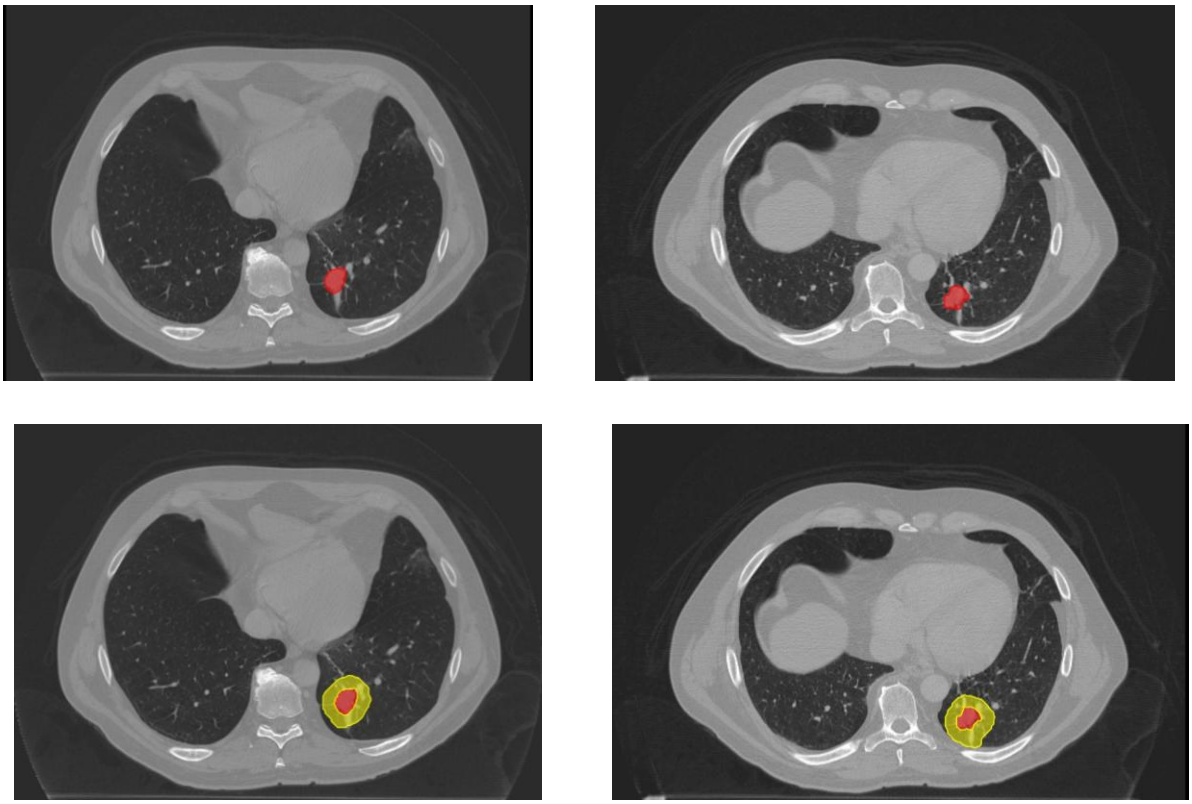

Figure 1. An axial view of a representative patient; (First row) delineated tumor and (second row) normalized ring for (left column) deep inhale and (right column) natural exhale for the purpose of elasticity calculation.

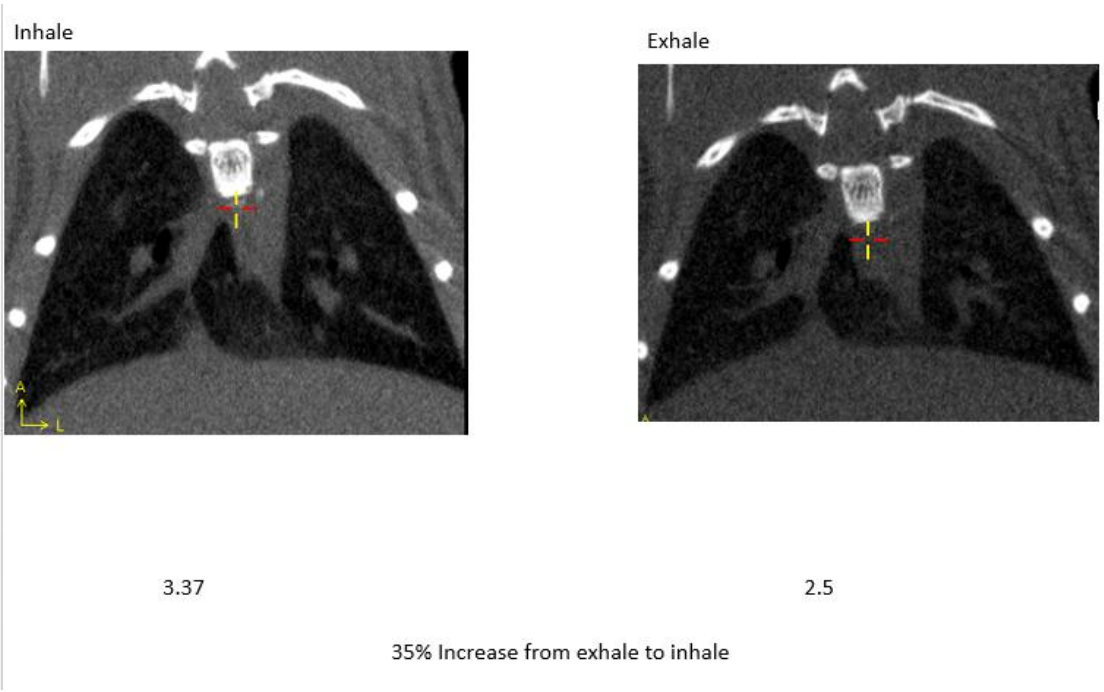

Figure 2: Gated CT images of the lung showing peak inhale and exhale for a representative rat. The numbers below the images refer to the volume of the lung in cc.

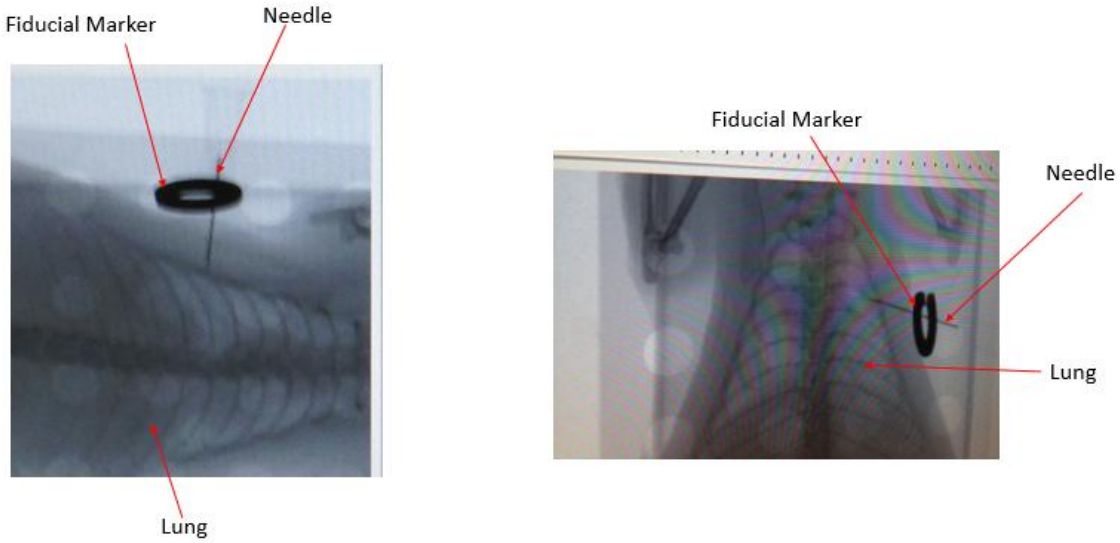

Figure 3: Fluoroscopy images from different gantry angles showing the tip of the needle near the lungs.

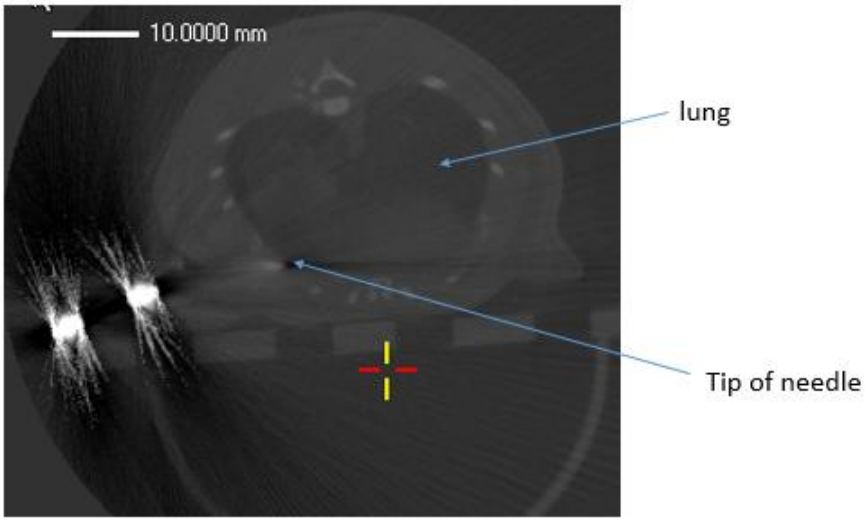

Figure 4: CT imaging showing the tip of the 1.2 cm needle near the lungs.

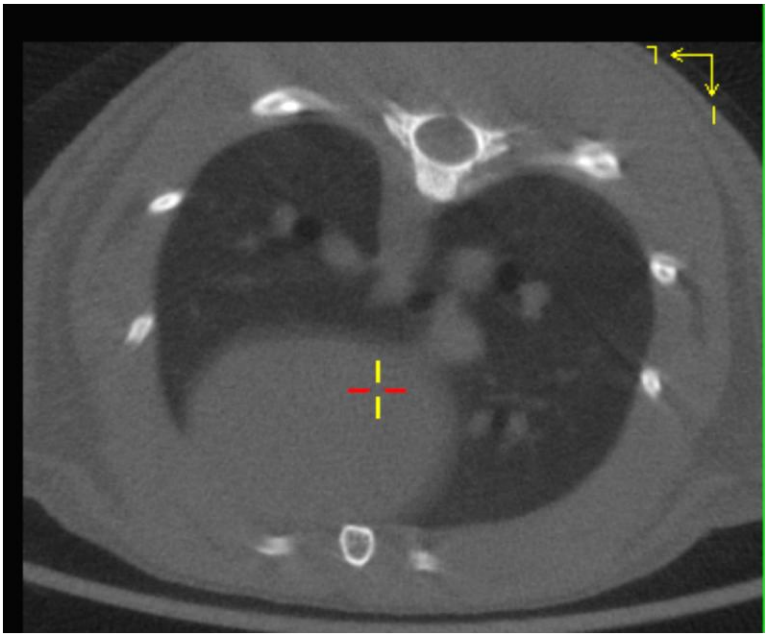

Figure 5: Axial CT image of the lung one month after implantation of the carbon particles. No granulomatous inflammation is observable.

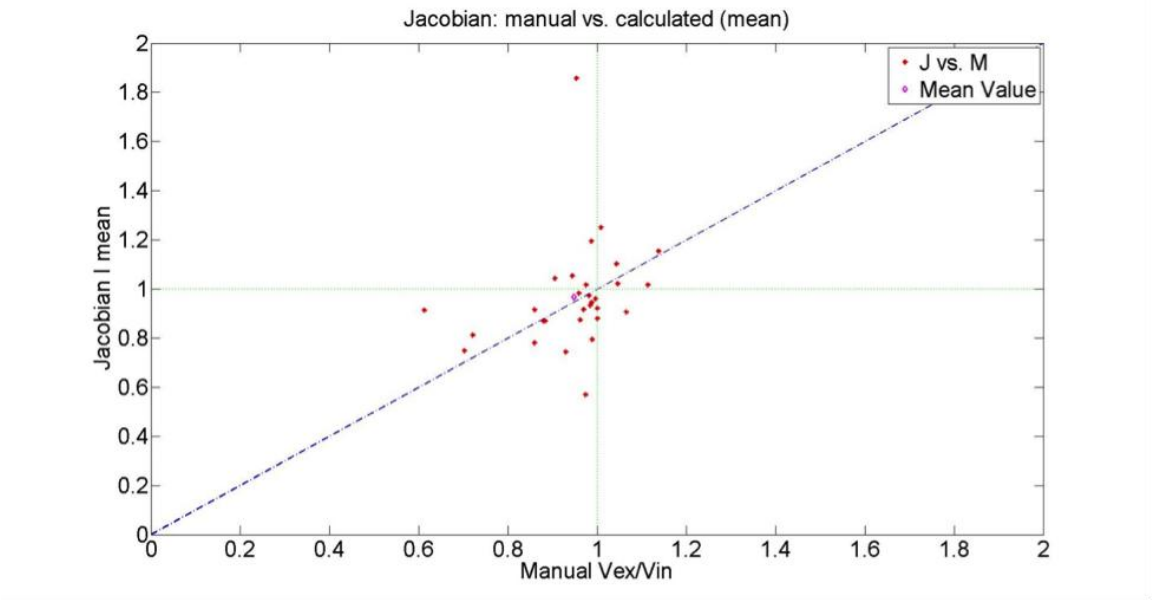

Figure 6: Linear regression analysis of the manual contouring method versus the calculated Jacobian of the deformation map of the CT images derived from inhale to exhale. (R^2=0.7, p=0.02)

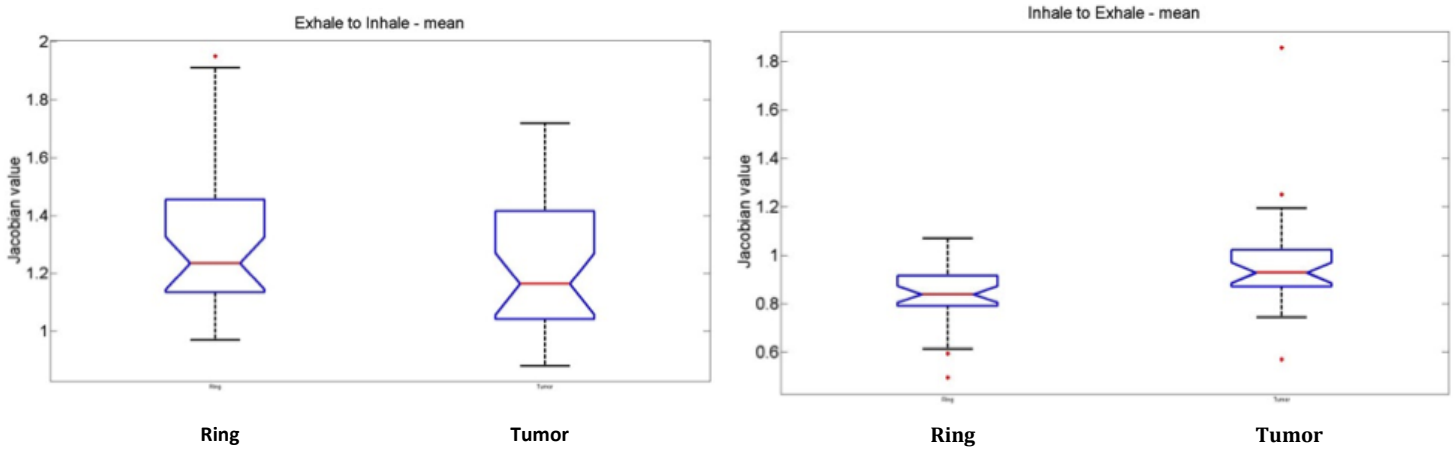

Figure 7: Box plot of the calculated Jacobian of the ring and PN for 30 examined patients. The central mark depicts the median values, the edges are the 25th and 75th percentiles and the whiskers extend to the extreme data points. (Left) Jacobian derived from exhale to inhale. (Right) Jacobian derived from exhale to inhale.

Abstract submitted to the Annual Conference of the AAPM:

Automated Tool for Determining Pulmonary Nodule Elasticity to Distinguish Malignant Nodules

Purpose: To develop and validate an automated method of determining pulmonary nodule (PN) elasticity against a manual contouring method, and preliminarily assess its ability to distinguish malignant tissue by comparing the elasticities of malignant PNs treated with stereotactic ablative radiotherapy (SABR) with those of the lung.

Methods: We analyzed breath-hold images of 30 patients with malignant PNs who underwent SABR in our department. A parametric nonrigid transformation model based on multi-level B-spline guided by Sum of Squared Differences similarity metric was applied on breath-hold images to determine the deformation map. The Jacobian of the calculated deformation map, which is directly related to the volume changes between the two respiratory phases, was calculated. Next, elasticity parameter will be derived by calculating the ratio of the Jacobian of the PN to the Jacobian of a 1cm region of lung tissue surrounding the tumor (E-ROI) as well as the Jacobian of the whole lung (E-Lung).

Results: For the first group of 15 patients we evaluated the volumetric changes of PNs and the lung from the maximum exhale phase to the maximum inhale phase, whereas the reverse was done for the second group of 15 patients. For the first group, mean and standard deviation for E-ROI and E-Lung were 0.91±0.09 and 0.86±0.18, respectively, which was verified by the manual method. For the second group, E-ROI and E-Lung were 1.34±0.27 and 1.57±0.51, respectively. These results demonstrate that the elasticity of the PNs was less than that of the surrounding lung ($p<0.0037$).

Conclusion: We developed an automated tool to determine the elasticity of PNs based on deformable image registration of breath-hold images. The tool was validated against manual contouring. Preliminarily, PN elastometry distinguishes proven malignant PNs from normal tissue of lung, suggesting its potential utility as a non-invasive diagnostic tool to differentiate malignant from benign PN.

Abstract submitted to the Annual Conference of the RSNA:

Automated Pulmonary Nodule Elastometry as a Potential Diagnostic Tool

Purpose/Objective(s): To validate an automated method of determining pulmonary nodule (PN) elasticity against a manual contouring method, and preliminarily assess its ability to distinguish malignant from benign tissue by comparing the elasticities of malignant PNs treated with stereotactic ablative radiotherapy (SABR) with those of the lung and of untreated PN without a definite malignant diagnosis.

Materials/Methods: We analyzed four dimensional computed tomography (4DCT) images of 30 patients with malignant PNs who underwent SABR in our department. A parametric nonrigid transformation model based on multi-level B-spline guided by Sum of Squared Differences similarity metric was applied on consecutive respiratory phases of 4D CT scans to determine the deformation map between inhale and exhale images. The Jacobian of the calculated deformation map, which is directly related to the volume changes between the two respiratory phases, was calculated. Next, the Jacobian of the tumor was normalized to the Jacobian of a 1cm region of lung tissue surrounding the tumor (NJ-ROI) as well as the Jacobian of the whole lung (NJ-Lung). Elasticity was defined as the volumetric change from one phase to the other. Secondly, the PNs were manually delineated on the inhale and exhale images and the volume changes of the PNs were compared to those calculated by our automated method.

Results: For the first group of 15 patients we evaluated the volumetric changes of the PNs and the lung from the maximum inhale phase to the maximum exhale phase, whereas the reverse was done for the second group of 15 patients. For the first group, mean and standard deviation for NJ-ROI and NJ-Lung were 0.91±0.09 and 0.86±0.18, respectively, which was verified by the manual method. For the second group, NJ-ROI and NJ-Lung were 1.34±0.27 and 1.57±0.51, respectively. These results demonstrate that the elasticity of the PNs was less than that of the surrounding lung ($p<0.0037$). Given this result, study was performed retrospectively. We then applied automated PN elastometry on 4DCT for five multifocal patients with multiple PNs. In each, at least one documented malignant PN (range 0.3-5.5) was treated with SABR along with averagely 2 suspicious sites (range 1-3) which have chosen to watch and additional PNs (range 0.2-8.4) without a definite malignant diagnosis. We found that the normalized Jacobian of treated tumors is averagely 16% (range 11%-24%) greater than normalized Jacobian of observed PNs ($p<0.034$).

Conclusions: We developed an automated tool to determine the elasticity of PNs based on deformable image registration of 4DCT images. The tool was validated against manual contouring. Preliminarily, PN elastometry distinguishes proven malignant PNs from untreated ones, suggesting its potential utility as a non-invasive diagnostic tool. This will need to be confirmed in a larger cohort of PNs with pathologic correlation.